A coordinated control strategy for battery/supercapacitor hybrid energy storage system to eliminate unbalanced voltage in a standalone AC microgrid

Received 25 August 2020
Revised 5 September 2020
Accepted 5 September 2020

Yaxing Ren
WMG, University of Warwick, Coventry, UK
Saqib Jamshed Rind
Department of Automotive and Marine Engineering, NED University of Engineering and Technology, Karachi, Pakistan, and
Lin Jiang
University of Liverpool, Liverpool, UK

Abstract

Purpose – A standalone microgrid (MG) is able to use local renewable resources and reduce the loss in long distance transmission. But the single-phase device in a standalone MG can cause the voltage unbalance condition and additional power loss that reduces the cycle life of battery. This paper proposes an energy management strategy for the battery/supercapacitor (SC) hybrid energy storage system (HESS) to improve the transient performance of bus voltage under unbalanced load condition in a standalone AC microgrid (MG).

Design/methodology/approach – The SC has high power density and much more cycling times than battery and thus to be controlled to absorb the transient and unbalanced active power as well as the reactive power under unbalanced condition. Under the proposed energy management design, the battery only needs to generate balanced power to balance the steady state power demand. The energy management strategy for battery/SC HESS in a standalone AC MG is validated in simulation study using PSCAD/EMTDC.

Findings – The results show that the energy management strategy of HESS maintains the bus voltage and eliminates the unbalance condition under single-phase load. In addition, with the SC to absorb the reactive power and unbalanced active power, the unnecessary power loss in battery is reduced with shown less accumulate depth of discharge and higher average efficiency.

Originality/value – With this technology, the service life of the HESS can be extended and the total cost can be reduced.

Keywords Energy management, Battery and supercapacitor, Hybrid energy storage system, Coordinated control, Unbalanced condition, Standalone microgrid

Paper type Research paper

1. Introduction

With the fast development of electrical technologies in recent decades, modern power systems normally use a lot of distributed resources (DRs), including both the renewable energy generations, such as wind turbine, photovoltaic (PV), geothermal and tidal, and micro resources, such as fuel cell and micro-turbine (Blaabjerg *et al.*, 2004). Apart from that, the

Journal of Intelligent Manufacturing and Special Equipment
Vol. 1 No. 1, 2020
pp. 3-23
Emerald Publishing Limited
e-ISSN: 2633-660X
p-ISSN: 2633-6596
DOI 10.1108/JIMSE-08-2020-0007

high-voltage direct current transmission and even the mixed usage of AC and DC networks also quick developed. These achievements make the development of power system use increasing more power electronics in power generation, transmission, distribution and end-user side (Blaabjerg *et al.*, 2013). Thus, the power-electronics-enabled power systems (PEEPS) has high potential to become the main solution in future power systems.

The PEEPS technologies have been used in some special applications, such as electric aircrafts (Maldonado and Korba, 1999; Rosero *et al.*, 2007; Wheeler and Bozhko, 2014), fuel cell ships (El-mezyani *et al.*, 2012) and low-voltage (LV) islanded microgrid (MG) (Lasseter, 2002; Peas Lopes *et al.*, 2006). However, as the power electronics based distributed resources are flexible and fast reaction in operation, it makes the PEEPS has less stiffness and inertia than the traditional power grids that use large generator as main sources (Diaz *et al.*, 2009; Guerrero *et al.*, 2011). In addition, because the power of renewable power generation is affected by the uncertainty of the weather and the randomness of end-user power consumption, it is difficult to ensure that power generation and power consumption can always be balanced. Therefore, when the renewable energy DR generates power less than the demand in the MG, alternative resources are needed as a backup power source.

The controllable micro-sources are chosen as the alternative resources for MG applications. The most common choices are micro-turbines and fuel cells. The micro-sources can response in seconds, which is faster than the traditional backup power sources, such as diesel engine. But it is still not fast enough for the low stiffness microgrid under disturbance. In addition, the micro-sources are transferring the chemical energy into electrical energy and its operation only support uni-directional power flow. Therefore, energy storage systems (ESS) are often required in PEEPS systems to ensure the balance of power generation and consumption. The most common ESSs include batteries, flywheels and super-capacitors (SC). Because of their fast response speed, bi-directional power flow characteristics and independency to weather conditions, they can be used independently to balance the power difference between the generation side and the demand side (Li *et al.*, 2010; Tummuru *et al.*, 2015; Zhou *et al.*, 2011; Zhang *et al.*, 2010).

As the two most commonly applied energy storage devices, the battery and SC have their own advantages and disadvantages. The battery has higher energy density but lower power density and less cycling life, normally up to several hundred cycles. The SC has higher power density and cycling life than battery but much lower energy density. Thus, the battery can be used as long time storing of energy while the SC can be used for short time high power supply and frequent energy recycling. A hybrid energy storage system (HESS) combining battery and SC then become a typical solution to provide both high energy capacities and high power density (Li and Joos, 2008a; Dogger *et al.*, 2011). In recent years, this application is widely applied in electric vehicle (Camara *et al.*, 2008, 2010, 2012; Zhang *et al.*, 2017; Golchoubian and Azad, 2017; Song *et al.*, 2017, 2018; Yodwong *et al.*, 2020), tramway (Han *et al.*, 2017; Li *et al.*, 2017), fuel cell ship (Chen *et al.*, 2020), wind/PV power generation system (Li *et al.*, 2010; Tummuru *et al.*, 2015; Abdelkader *et al.*, 2018; Jing *et al.*, 2018), other renewable energy sources (Jayasinghe *et al.*, 2011) and DC microgrid (Thounthong *et al.*, 2007; Zhou *et al.*, 2011; Jing *et al.*, 2016; Enang and Johnson, 2020).

The LV DC network has some disadvantages of its low efficiency in long distance power transmission and requires large number of DC/AC converters to join distribution AC network. A typical AC microgrid normally with components of renewable power generation, energy storage, and power consumptions, as shown in Figure 1. In order to use LV DC energy storage devices in the AC microgrid, the coordinated control of the HESS is required to transfer their characteristics from DC to AC. As the power of renewable energy is unpredictable and changes rapidly with weather conditions, a large number of DRs used in MG will cause frequent charge and discharge cycles on ESS. As the battery usually has only hundreds of cycles of life, if the battery is only sources in ESS to balance the power of the DR and the load in

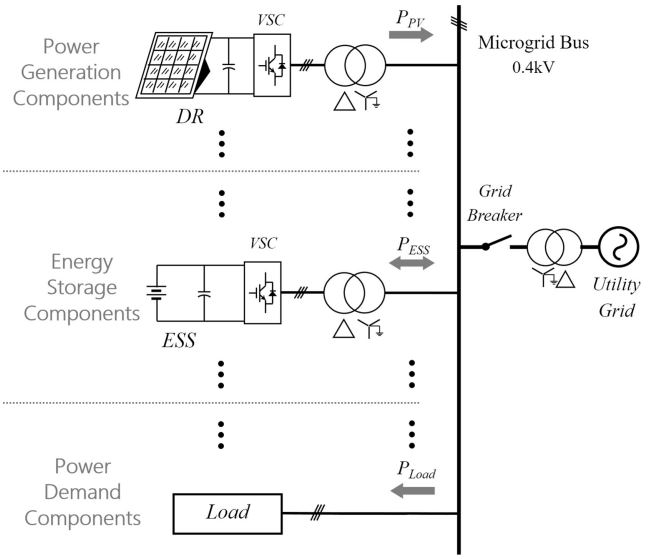

Figure 1.
Scheme of a typical microgrid

the MG, the cumulative depth of discharge (DOD) will increase rapidly, resulting in battery aging and reduction in cycle life (Li and Joos, 2008a). To solve this, many researchers have proposed the methods of using batteries and SCs together in a hybrid energy storage system (HESS). Some literatures have proposed HESS control strategies in microgrids, such as using Fourier Transform to decompose the frequency information of load power to allocate load power to batteries and SCs (Mao *et al.*, 2013); or use SC to compensate the harmonics and imbalance of battery current output to improve power quality (Zhu *et al.*, 2014).

However, in actual application of MG, the power consumption and generation are not three-phase balanced. Most power consumption devices, such as washing machines, and power generation systems, such as PVs, are connecting directly to a single-phase AC power line. This causes the high risk of three-phase unbalance conditions in AC bus in Microgrid. The previous control strategies have not been designed to control the battery and SC individually with different purposes for optimizing their usage efficiency based on their features. The control strategies for battery and supercapacitor should be designed to coordinate their performances under the unbalance condition considering the low stiffness feature of a standalone AC microgrid (Ren *et al.*, 2016).

This paper proposes an energy management strategy for the battery/SC HESS in order to improve the transient response of the MG bus voltage and reduce the accumulate DOD of battery under unbalanced voltage conditions. The SC is controlled to absorb the transient and unbalanced active power as well as the reactive power, while the battery is controlled only generate balanced power for the steady state power demand. Thus, the power oscillation caused by unbalanced voltage condition will be compensated by SC and this unnecessary power loss can be eliminated from the battery to reduce the accumulate DOD and thus increase the battery usage period.

2. Model of energy storage system in microgrid

2.1 Battery model and state of charge

In recent decades, with the popularity of Li-ion battery, the modelling of battery has been widely researched. There are two main categories of battery models, the electrochemical

model, and the equivalent circuit model. The electrochemical model represents the behaviour of internal chemical reaction with modelling the movement of electrons. This type of model includes detailed information of battery and can be used to predict the performance, aging, thermal behaviour, and even failure rate of battery cells. However, these models are very complex and with extremely high orders, most are more than three hundred orders (Li *et al.*, 2019). To simplify the model of battery, the equivalent circuit model uses the ideal battery, resistor, and capacitance to emulate the electrical behaviour of battery. Thus, the parameters of equivalent circuit model have no direct relationship with physical components inside the battery cells. And it is difficult to use the equivalent circuit model to simulate the aging and thermal behaviour of battery (Hu *et al.*, 2011). This paper uses the electrical equivalent circuit model of battery that neglecting the temperature impact and battery aging performance.

The terminal voltage of a battery is presented from the Thevenin battery model as shown in Figure 2a. The ideal battery model is used to present the open circuit voltage (OCV) V_{ocv}. Battery OCV is corresponding to its state of charge (SOC), which is normally defined as the integration of charging current to presents the power absorbed by battery or produced from the battery (Bae *et al.*, 2014). The power loss during battery operating is presented by the battery discharging current I flow through an internal resistance R_i. It transient behaviour referring to the varying load is presented by a parallel RC circuit with a transient contact resistor R_T and capacitor C_T whose voltage is known as V_T. The dynamics of battery equivalent circuit model can be presented as (Tremblay *et al.*, 2007)

$$V_{\text{batt}} = V_{\text{OC}} - R_i \cdot I - V_T \tag{1}$$

where

$$V_{\text{OC}} = E_0 - K\frac{Q_0}{Q_0 - \int idt} + Ae^{\left(-B\cdot\int Idt\right)} \tag{2}$$

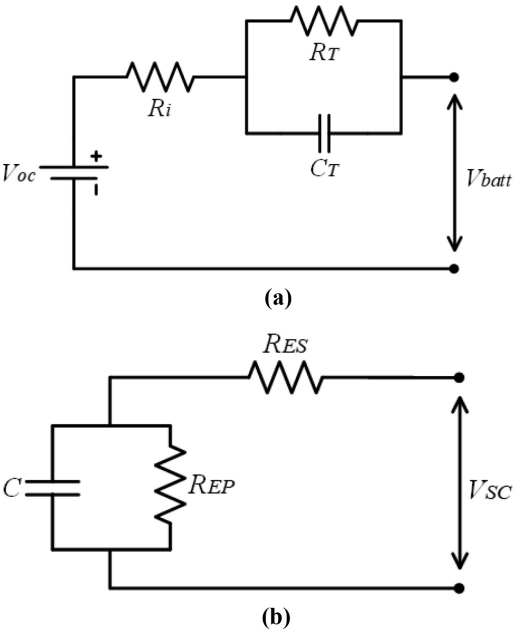

Figure 2.
Equivalent circuit of (a) battery, and (b) supercapacitor

$$V_T = \frac{1}{C_T}\int\left(I - \frac{V_{CT}}{R_T}dt\right) \tag{3}$$

where E_0 is the nominal open circuit voltage of battery, Q_0 is the rated capacity of battery in Coulomb, the integration of current. This paper does not consider the battery aging, which decreases the battery fully charged capacity and voltage. Thus E_0 and Q_0 are set as constant value. K is the polarization voltage, A is the exponential amplitude and B is the related time constant (Tremblay *et al.*, 2007). The parameters are varying referring to different battery types. The battery SOC and DOD are presented as (Dogger *et al.*, 2011)

$$\text{SOC} = \frac{Q}{Q_0} \tag{4}$$

$$\text{DOD} = \Delta\text{SOC} = \frac{1}{Q_0}\int I(t)dt \tag{5}$$

2.2 Supercapacitor model

The SC has the feature of very fast charging and discharging speed that can reach its peak current immediately as a conventional capacitor and with a very large capacity than conventional capacitor (Abbey and Joos, 2007). In addition, similar with traditional capacitors, the SC has much higher self-discharging rate than battery. Even without external load, it can self-discharge to consume one-third its stored energy within a month of time. Thus, it is normally only used for short-term power exchange.

As the electrical behaviour of SC is similar with a capacitor, its main component is a fixed value ideal capacitor. Its self-discharge behaviour is presented by an equivalent parallel resistor (EPR). The SC can be model by a RC loop and an equivalent series resistance (ESR) as shown in Figure 2b, accurately without considering the effect by temperature and other operation conditions (Li and Joos, 2008b). The dynamic model of SC is presented as

$$V_{\text{sc}} = V_c - \frac{1}{C}\int\left(i_C - \frac{V_{\text{sc}}}{R_{\text{EP}}}\right)dt - R_{\text{ES}}\cdot i_C \tag{6}$$

where V_{sc} is the terminal voltage of SC, V_c is its initial open circuit voltage depending on its state of charge, i_C is the discharging current, C is the capacitance of SC, R_{EP} and R_{ES} are the equivalent parallel and series resistor of SC.

2.3 Model of voltage source converter (VSC)

The voltage source converters (VSCs) are used to inverse the DC voltage of ESS to synchronize the AC voltage of bus in the MG. The VSC will need to be controlled to regulate the current flowing into the inductors and transfer it between DC format and AC format. The normal modulation methods of VSC are pulse-width-modulation or space-vector modulation. Thus, it needs a filter loop to smooth the PWM current flowing from the ESS into a sinewave current. This paper uses the VSC model with a LC filter in *d-q* axis as (Mohamed and El-Saadany, 2008; Bidram *et al.*, 2013)

$$\frac{di_{\text{Ld}}}{dt} = -\frac{R_s}{L_s}i_{\text{Ld}} + \omega i_{\text{Lq}} - \frac{1}{L_s}v_{\text{od}} + \frac{1}{L}v_{\text{d}} \tag{7}$$

$$\frac{di_{\mathrm{Lq}}}{dt} = -\frac{R_s}{L_s} i_{\mathrm{Lq}} - \omega i_{\mathrm{Ld}} - \frac{1}{L_s} v_{\mathrm{oq}} + \frac{1}{L} v_q \tag{8}$$

$$\frac{dv_{\mathrm{od}}}{dt} = \omega v_{\mathrm{oq}} + \frac{1}{C_s} i_{\mathrm{Ld}} - \frac{1}{C_s} i_{\mathrm{od}} \tag{9}$$

$$\frac{dv_{\mathrm{oq}}}{dt} = -\omega v_{\mathrm{od}} + \frac{1}{C_s} i_{\mathrm{Lq}} - \frac{1}{C_s} i_{\mathrm{oq}} \tag{10}$$

where v_{od}, v_{oq}, i_{od}, i_{oq}, are the output voltage and current in d- and q-axis, respectively. i_{Ld}, i_{Lq}, are the currents flow into the inductor L_s. v_d and v_q are the control output voltage reference in d- and q- axis. ω is the synchronous electrical angular speed in the AC voltage for Park transformation. R_s, L_s and C_s are the resistance, inductance and capacitance of the VSC.

2.4 Power efficiency and voltage unbalance factor

The power loss on resistance of either battery or converter can reduce the total efficiency of the HESS system. The power consumption on the battery internal resistance will not only decrease the efficiency but also increase the ambient temperature that causes more risks in battery failure. The efficiency of the whole HESS system during charge and discharge cycles is defined as

$$\eta_{\mathrm{charge}} = \frac{P_{\mathrm{stored}}}{P_{\mathrm{input}}} \tag{11}$$

$$\eta_{\mathrm{discharge}} = \frac{P_{\mathrm{output}}}{P_{\mathrm{generated}}} \tag{12}$$

To combine the charging and discharging efficiency in one equation, the efficiency can be represented by the ratio between the min value and the max value of battery terminal power and cell power as

$$\eta_{\mathrm{battery}} = \frac{\min(|P_{\mathrm{cell}}|, |P_{\mathrm{term}}|)}{\max(|P_{\mathrm{term}}|, |P_{\mathrm{cell}}|)} \tag{13}$$

Under unbalanced load condition, the voltage of AC bus is not balanced as a perfect three-phase sinewave. The index of presenting the level of unbalance condition is using the voltage unbalance factor (VUF). The VUF is defined as the ratio of the negative-sequence component over the positive-sequence component of the target voltage waveform as (Savaghebi *et al.*, 2013):

$$\mathrm{VUF} = \frac{v^{-}_{b(\mathrm{RMS})}}{v^{+}_{b(\mathrm{RMS})}} \times 100\% \tag{14}$$

where $v^{+}_{b(\mathrm{RMS})}$ and $v^{-}_{b(\mathrm{RMS})}$ are the root-mean-square (RMS) value of positive- and negative-sequences of bus voltage in AC grid.

3. Energy management strategy for HESS

The proposed energy management strategy with coordination control of battery and SC is designed to use the supercapacitor (SC) to generate transient unbalance power for eliminating the unbalanced voltage in the AC bus. The control strategy of HESS aims to improve the

transient performance of MG bus voltage under unplanned sudden load, or generation, and reduce the battery power loss under unbalance condition.

The energy management strategy controls the battery to provide the three-phase balanced current to balance the steady-state power demand. And the SC is controlled to compensate the unbalanced power demand, provide the reactive power and transient power demand before the battery reaches the steady state. Then the oscillated power caused by unbalanced voltage is compensated by the SC with the mean energy of zero to avoid the battery to perform the frequent recharging that reduces its accumulate DOD and cycle life.

3.1 Controller for battery VSC

In the battery/SC HESS, the battery aims to generate three-phase balanced power under unbalanced voltage condition. Thus, the control algorithm of battery extracts the positive components of bus voltage and generate the current reference to synchronize with the positive-sequence bus voltage with power factor equal to one

$$i_{d+}^{*} = \left(k_p + \frac{k_i}{s}\right)(v_{\text{dref}} - v_{\text{od}+}) - \omega C_s v_{\text{oq}+} \tag{15}$$

$$i_{q+}^{*} = \left(k_p + \frac{k_i}{s}\right)(v_{\text{qref}} - v_{\text{oq}+}) + \omega C_s v_{\text{od}+} \tag{16}$$

When the unbalanced condition happens, in order to decouple the positive and negative sequence components, the common method is to synchronize them in the same frequency but opposite direction. Rotate the positive-sequence frame under the frequency of ω and the negative-sequence frame under the frequency of $-\omega$. Then at the rotating frame synchronizing to the positive-sequence, the negative-sequence components voltages and currents are presented with double fundamental frequency in opposite direction as -2ω.

The instantaneous active power is presented as

$$\begin{aligned} p &= v_{\text{od}}\, i_d + v_{\text{oq}}\, i_q \\ &= (v_{\text{od}+} + v_{\text{od}-})(i_{d+} + i_{d-}) + (v_{\text{oq}+} + v_{\text{oq}-})(i_{q+} + i_{q-}) \\ &= \underbrace{v_{\text{od}+}\, i_{d+} + v_{\text{oq}+}\, i_{q+} + v_{\text{od}-}\, i_{d-} + v_{\text{oq}-}\, i_{q-}}_{P} \\ &\quad \underbrace{+ v_{\text{od}+}\, i_{d-} + v_{\text{od}-}\, i_{d+} + v_{\text{oq}+}\, i_{q-} + v_{\text{oq}-}\, i_{q+}}_{\tilde{p}} \end{aligned} \tag{17}$$

where P presents the average power and $\tilde{p}$ presents the oscillation power flowing into the grid; $v_{\text{od}+}$, $v_{\text{oq}+}$, $v_{\text{od}-}$ and $v_{\text{oq}-}$ are the positive- and negative-sequence components of bus voltage in d-q frame; i_{d+}, i_{q+}, i_{d-} and i_{q-} are the positive- and negative-sequence components of output current in d-q frame flowing from energy storage device to the grid.

To eliminate the power oscillation, let $\tilde{p} = 0$, and assume $v_{\text{oq}+} = 0$ in steady state. Then the negative-sequence output current in d-axis can be presented as

$$i_{d-} = -\frac{v_{\text{od}-}}{v_{\text{od}+}}\, i_{d+} - \frac{v_{\text{oq}-}}{v_{\text{od}+}}\, i_{q+} \tag{18}$$

Then the reference d-axis current reference can be designed as

$$i_d^{*} = i_{d+}^{*} + i_{d-}^{*} = \left(1 - \frac{v_{\text{od}-}}{v_{\text{od}+}}\right) i_{d+}^{*} - \frac{v_{\text{oq}-}}{v_{\text{od}+}}\, i_{q+}^{*} \tag{19}$$

Similarly, the instantaneous reactive power can be obtained as

$$q = \underbrace{v_{\mathrm{oq}+}\, i_{d+} - v_{\mathrm{od}+}\, i_{q+} + v_{\mathrm{oq}-}\, i_{d-} + v_{\mathrm{od}-}\, i_{q-}}_{Q} + \underbrace{v_{\mathrm{oq}-}\, i_{d+} - v_{\mathrm{od}-}\, i_{q+} + v_{\mathrm{oq}+}\, i_{d-} - v_{\mathrm{od}+}\, i_{q-}}_{\tilde{q}} \tag{20}$$

and the reference q-axis current can be designed as

$$i_q^* = i_{q+}^* + i_{q-}^* = \left(1 - \frac{v_{\mathrm{od}-}}{v_{\mathrm{od}+}}\right) i_{q+}^* + \frac{v_{\mathrm{oq}-}}{v_{\mathrm{od}+}}\, i_{d+}^* \tag{21}$$

The reference current of the battery VSC is presented as

$$\begin{bmatrix} i_d^* \\ i_q^* \end{bmatrix} = \begin{bmatrix} 1 - \dfrac{v_{\mathrm{od}-}}{v_{\mathrm{od}+}} & -\dfrac{v_{\mathrm{oq}-}}{v_{\mathrm{od}+}} \\ \dfrac{v_{\mathrm{oq}-}}{v_{\mathrm{od}+}} & 1 - \dfrac{v_{\mathrm{od}-}}{v_{\mathrm{od}+}} \end{bmatrix} \times \begin{bmatrix} i_{d+}^* \\ i_{q+}^* \end{bmatrix} \tag{22}$$

The controller block diagram of energy management strategy for battery system is shown in Figure 3a.

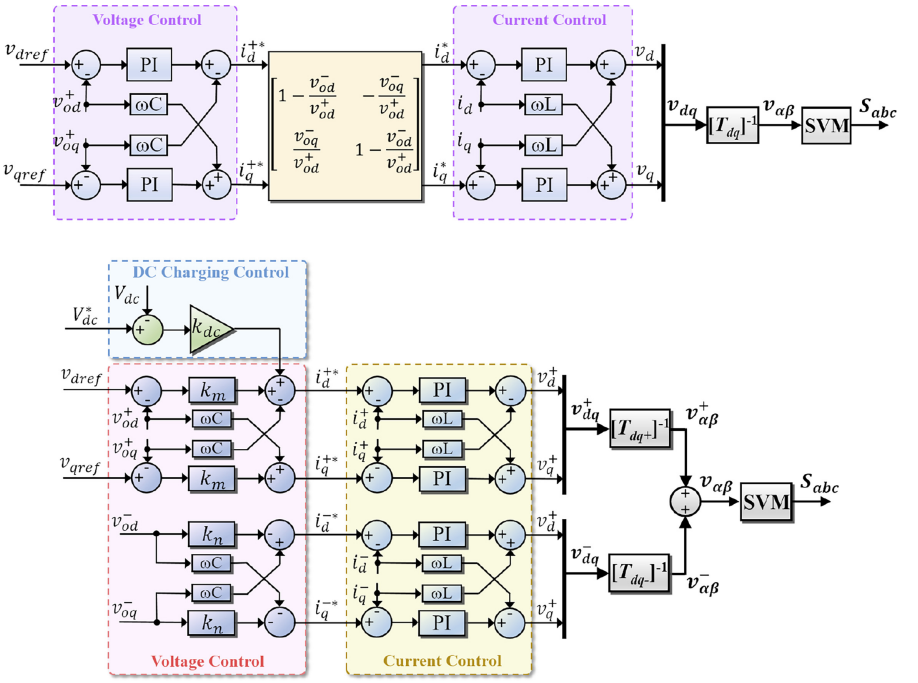

Figure 3.
Control block diagram of HESS for (a) battery and (b) supercapacitor

3.2 Controller for VSC of supercapacitor

As SC is a high-power density device storing less energy capacity, it is not used for long-term (tens of minutes or hours) power supply. The functionality of SC in the HESS is to balance the transient high-power demand. Therefore, the proportional gain is used in the positive-sequence voltage and current regulation for a rapid dynamic response.

In addition, as its low energy capacity feature, it is necessary to avoid the over voltage and under voltage issue of the SC. This aims to maintain the performance of SC via recharging it to its nominal voltage level. Therefore, additional charging loop should be added on the energy management strategy. The current control is designed under the dual synchronous reference frames (SRF), which splits the positive- and negative-sequence components in different frames. The control algorithm is presented as

$$i_{d,\mathrm{sc}}^{+*} = k_m(v_{\mathrm{dref}} - v_{\mathrm{od}+}) - \omega C_s v_{\mathrm{oq}+} + k_{\mathrm{dc}}\left(V_{\mathrm{sc}} - V_{\mathrm{sc}}^{*}\right) \tag{23}$$

$$i_{q,\mathrm{sc}}^{+*} = k_m(v_{\mathrm{qref}} - v_{\mathrm{oq}+}) + \omega C_s v_{\mathrm{od}+} \tag{24}$$

$$i_{d,\mathrm{sc}}^{-*} = -k_n\, v_{\mathrm{od}-} + \omega C_s\, v_{\mathrm{oq}-} \tag{25}$$

$$i_{q,\mathrm{sc}}^{-*} = -k_n\, v_{\mathrm{oq}-} - \omega C_s\, v_{\mathrm{od}-} \tag{26}$$

where $i_{d_s c+}^{*}$ and $i_{q_s c+}^{*}$ are the positive-sequence reference current in d-q frame with synchronizing frequency at ω; $i_{d_s c-}^{*}$ and $i_{q_s c-}^{*}$ are the negative-sequence reference current in d-q frame with synchronizing frequency at $-\omega$; k_m and k_n are the proportional control gain for positive- and negative-sequence voltages; k_{dc} is the charging gain of SC to maintain its voltage.

The current references generated above are feeding an inner current loop that uses PI controllers to regulate output current tracking its reference. Then transfer the control output back into stationary frame using inverse Part's transformation, the final control output can be presented as

$$\begin{aligned}\begin{bmatrix} v_\alpha \\ v_\beta \end{bmatrix} &= T_{\mathrm{dq}^+}^{-1}\begin{bmatrix} v_{d+} \\ v_{q+} \end{bmatrix} + T_{\mathrm{dq}^-}^{-1}\begin{bmatrix} v_{d-} \\ v_{q-} \end{bmatrix} \\ &= \begin{bmatrix} \cos(\theta) & -\sin(\theta) \\ \sin(\theta) & \cos(\theta) \end{bmatrix}\begin{bmatrix} v_{d+} \\ v_{q+} \end{bmatrix} \\ &+ \begin{bmatrix} \cos(\theta) & \sin(\theta) \\ -\sin(\theta) & \cos(\theta) \end{bmatrix}\begin{bmatrix} v_{d-} \\ v_{q-} \end{bmatrix}\end{aligned} \tag{27}$$

where v_α, v_β are the reference voltage in stationary frame, v_{d+}, v_{q+}, v_{d-} and v_{q-} are the reference voltage in positive- and negative-sequence d-q frame; $T_{\mathrm{dq}+}^{-1}$ and $T_{\mathrm{dq}-}^{-1}$ are the inverse Park transformation. Finally, the space vector modulation (SVM) is used to produce switching signals to drive the VSC. The control block diagram of energy management strategy for SC system is shown in Figure 3b.

4. Simulation results

The designed energy management strategy is validated on a battery/SC hybrid system in a standalone MG, as the power stage shown in Figure 4, which is modelled and simulated in PSCAD/EMTDC software. To validate the energy management system that controls battery and SC in different objectives, the simulation cases are designed to test the coordinative operation performance of the HESS under unbalanced disturbance, including the single-phase impedance load and variable power generation. The parameters of the target LV AC

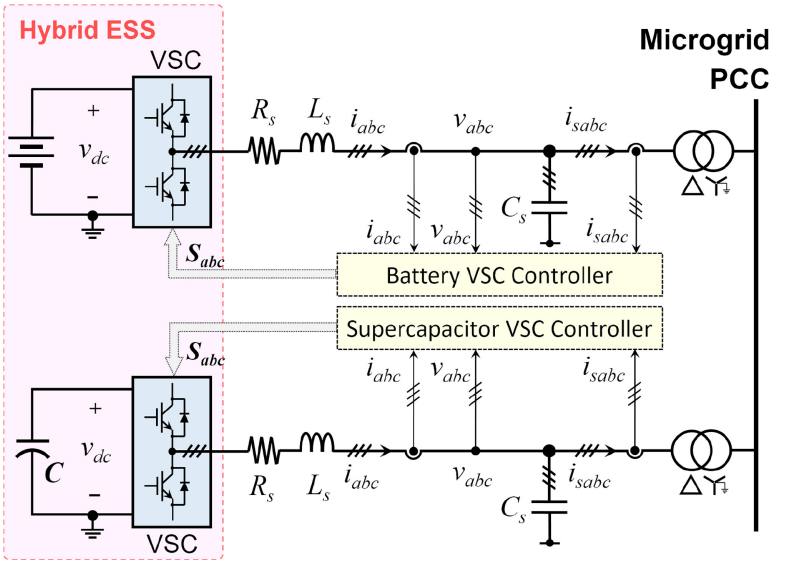

Figure 4.
The converter based hybrid ESS power stage

MG are given in Table 1, and the control parameters of the energy management system are given in Table 2.

4.1 Flexible combination of energy and power capacity

Under the sudden single-phase load, the grid bus voltage drops and show obvious unbalance condition. Figure 5a shows the bus voltage waveform under single-phase resistive load disturbance. To show the indices of the bus voltage rather than the three-phase waveform, the

System	Parameters	Symbol and value
MG	Line-to-line bus voltage	$v_b = 0.4\,\text{kV}$
	Bus frequency	$f_b = 50\,\text{Hz}$
Battery	Nominal voltage	$E_0 = 480\,\text{V}$
	Internal resistance	$R_i = 0.005\,\Omega$
	Transient contact resistance	$R_T = 0.0052\,\Omega$
	Transient contact capacitance	$C_T = 0.52\,\text{F}$
	Polarization voltage	$K = 0.00876\,\text{V}$
	Exponential amplitude	$A = 0.468\,\text{V}$
	Exponential time constant	$B = 3.529\,\text{A h}^{-1}$
	Rated capacity	$Q_0 = 2{,}800\,\text{Ah}$
	Initial SOC	50 %
SC	Nominal voltage	$V_{sc0} = 400\,\text{V}$
	Equivalent parallel resistance	$R_{EP} = 0.6\,\Omega$
	Equivalent series resistance	$R_{ES} = 120\,k\Omega$
	Capacitance	$C = 0.58\,\text{F}$
VSC	PWM frequency	$f_{PWM} = 2\,kHz$
	Filter inductance - per phase	$L_s = 2.4\,\text{mH}$
	Filter resistance - per phase	$R_s = 1\,\text{m}\Omega$
	Filter capacitance - per phase	$C_s = 290\,\mu\text{F}$

Table 1.
Parameters of MG and HESS

line-to-line bus voltage in RMS and voltage unbalance factor (VUF) is shown to indicate the performance of bus voltage, as in Figures 5b and c.

As the power capacity of the plug-and-play DRs and load depend on the customers in the MG, the ESS in the MG also need the ability of plug-and-play flexibility in combination of energy and power capacity. One superiority of the energy management method is the flexible design of the energy and power capacity. As an example of the HESS application, if the MG scheme is designed for an industry region, more power density is required for large number of

Source	Voltage control	Current control
Battery	$k_p = 0.5$ $k_i = 50$	$k_p = 5$ $k_i = 1{,}000$
SC	$k_m = 20$ $k_p = 50$ $k_{dc} = 5$	$k_p = 5$ $k_i = 1{,}000$

Table 2.
Controller parameters of HESS

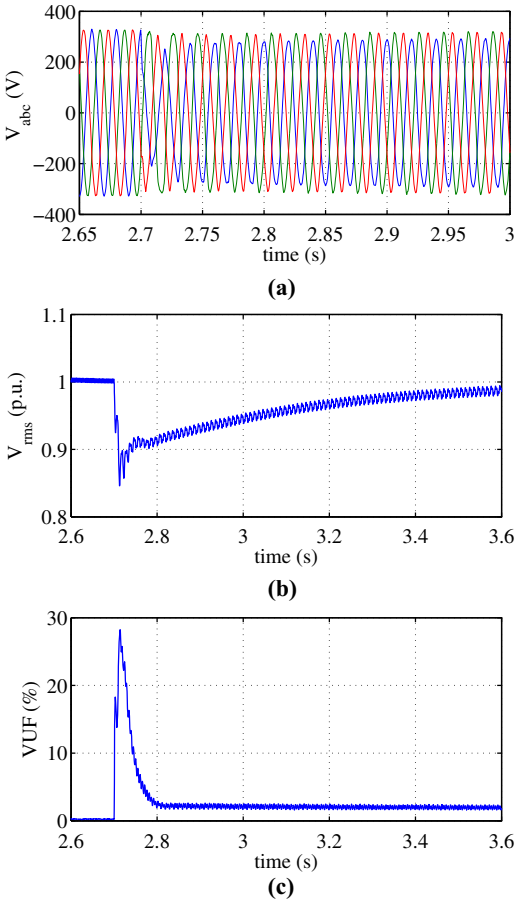

Figure 5.
Bus voltage transient performance under single phase load. (a) Bus voltage, (b) RMS voltage, (c) voltage unbalance factor.

induction motors (IM) used in industry. Due to the weak stiffness and inertia of MG, the frequent starting-up of high-power IMs is a huge impact to the MG and need more SC for transient power response. And if the MG is designed for residential region, only low-power devices are used. Then the energy capacity is more significant for continuous operation.

To compare between different energy and power capacities in flexible design of the HESS, different number of SCs are used to find out the performance improvement in bus voltage response. Thus, the pure battery ESS, and the HESSs include a battery and 1, 2, or 3 SCs are compared under the same system conditions and disturbances. The simulation compared under three-phase resistive load connected and disconnected, induction motor starting-up and single-phase load connected.

When sudden resistive load connected to the MG, the load absorbs power from grid. If the transient power generation is less than the power demand, the bus voltage will drop to reduce the power drain from grid to the load. Simulation results of sudden resistive load connected and disconnected with different number of SCs are shown in Figures 6a and c. Without the support of SC, the battery based ESS cannot provide power fast enough to follow the power demand. If using SC, the bus voltage drop is only one-third the drop of using pure battery ESS. Figure 6b shows the bus voltage response during inductive load connected. The performance improvement of using SC is faster in transient power generation. Figure 6d shows the bus voltage response under single-phase load. Because of the battery output power control is designed without unbalance voltage eliminate ability. If only uses the battery in the ESS, the bus voltage has oscillation under single-phase load has oscillation. The results show that with increasing number of SC, the bus voltage has increasing faster transient response in all load conditions.

Under the sudden load disturbance, the three-phase bus voltage will have transient unbalance condition referring to its phase angle. The VUF under previous disturbance is shown in Figure 7. As the result in Figures 7a–c shows the VUF of bus voltage under three phase load changes, the voltage unbalance condition are transient and will disappear at

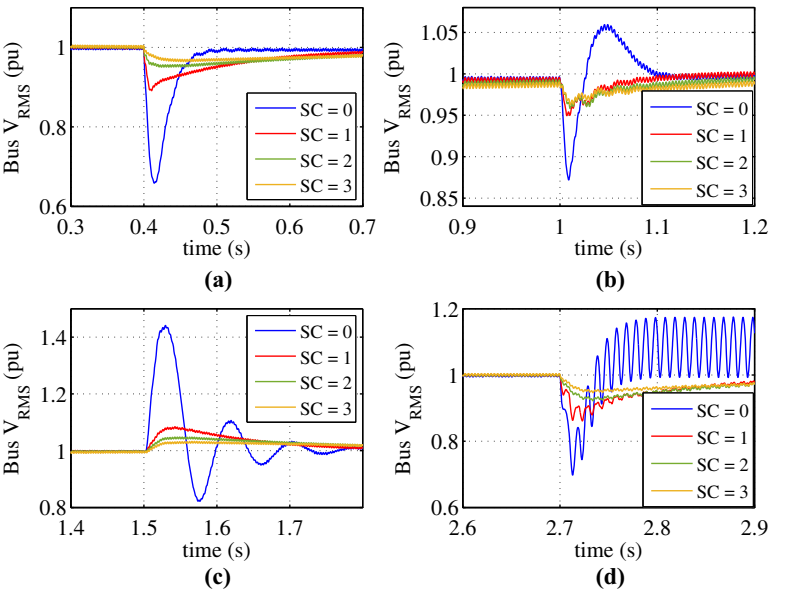

Figure 6.
Bus RMS voltage (p.u.) compare with different number of SCs under (a) resistive load connected, (b) inductive load connected, (c) resistive load disconnected, (d) single-phase load connected

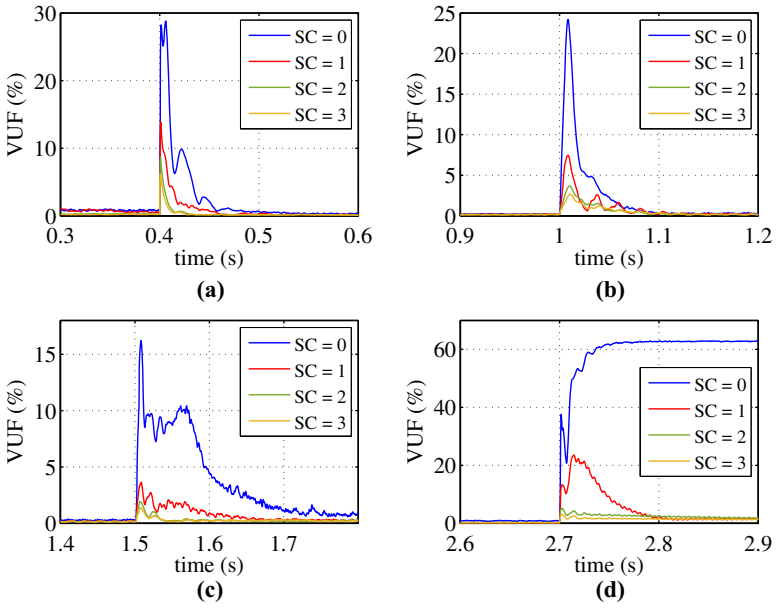

Figure 7.
VUF compare with different number of SCs under (a) resistive load connected, (b) inductive load connected, (c) resistive load disconnected, (d) single-phase load connected

steady state. From the result, it is obviously to find that the usage of SC can improve the transient performance in both the RMS bus voltage and VUF elimination. Under the single-phase load condition, the voltage unbalance condition will be continuous in both the transient response and in steady state. The energy management strategy of SC with unbalance elimination algorithm is able to reduce both the transient peak VUF and the steady state VUF as shown in Figure 7d. The result also indicates that the greater number of SC in use, the quicker the VUF at bus voltage will be eliminated. That validates the plug-and-play performance of the HESS system using the proposed energy management strategy. With this design, the usage of SC can be flexible referring to different objectives in the AC MG application.

4.2 Case 1: single-phase impedance load

The negative-sequence voltage components in bus voltage caused by unbalanced disturbance can cause more power loss in the ESS. The unwanted power loss leads more accumulated DOD in battery and that will reduce the battery cycle life. The designed energy management strategy aims to use SC absorbing the unbalance power for reducing the unnecessary accumulated DOD of battery and enhance the average efficiency.

Comparing the HESS with energy management strategy with battery only ESS, the proposed method has obvious improvement in bus voltage maintenance. The comparison of bus voltage waveform between the battery ESS and hybrid ESS are shown in Figures 8a and b. When the single-phase impedance load connects to the bus voltage of AC MG, the bus voltage drops immediately due to the sudden load. In the HESS with proposed energy management strategy, the SC responds first to produce transient power to compensate the unbalanced power demand. Then the battery slowly increases the output balanced power to tracking the steady state power demand and charging the SC back to its nominal voltage level. The results show the real voltage in three-phase sinewave directly. It can clearly show the difference but not easy to compare them to find the numerical improvements.

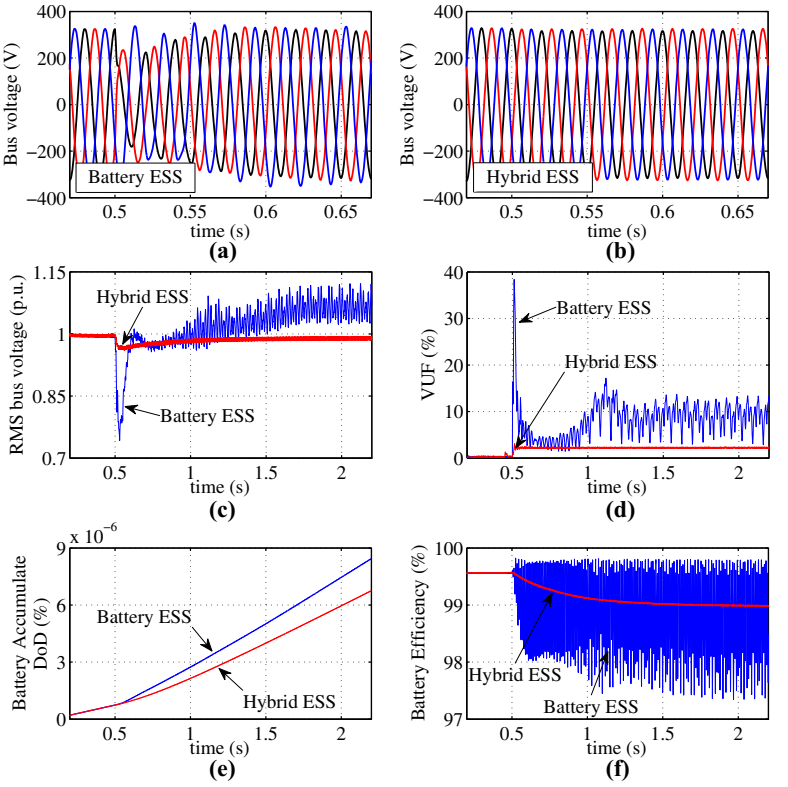

Figure 8.
Simulation comparison between battery ESS and hybrid ESS in a standalone microgrid under single phase load. (a) Bus voltage with battery ESS; (b) bus voltage with hybrid ESS; (c) comparison of RMS bus voltage; (d) bus voltage unbalance factor; (e) battery accumulate DOD; and (f) battery efficiency

Thus, the RMS voltage that indicates the voltage magnitude performance and VUF that indicates the voltage unbalance performance have been compared in Figures 8c and d.

The active power and reactive power comparison is shown in Figures 9a and b. From which it is easy to find that the SC produced the full reactive power while the battery produces the active power in steady state. This is to take the advantage of SC with its much more cycle life to avoid the battery frequent discharging cycles under unbalance voltage condition. To compare the current outputs, Figures 9c and d show the three-phase output current generated from the battery and SC separately using the energy management strategy. The current generated from battery is three-phase balanced and slowly increased to its steady state. And that from SC is obviously unbalanced to compensate the unbalanced power flow in the bus caused by single-phase load.

When single-phase load connected to the grid, the power is provided by the ESS to balance the power demand. In the battery ESS, the battery is the only sources to provide the unbalanced power to the single-phase load. This causes the unbalanced voltage on grid and then power oscillation in the battery. Figure 8e shows the battery accumulated DOD that indicates the usage of battery and Figure 8f shows the battery efficiency under the single-phase load. One can find that the battery efficiency has obvious oscillation cause by unbalanced condition. But in the hybrid ESS with proposed control strategy, the SC is designed to support the unbalanced power and charging itself from battery. Thus, in the hybrid ESS, it can be known that the SC is used to absorb the three-phase balanced power from battery and support the single-phase power to load as an energy buffer. From the

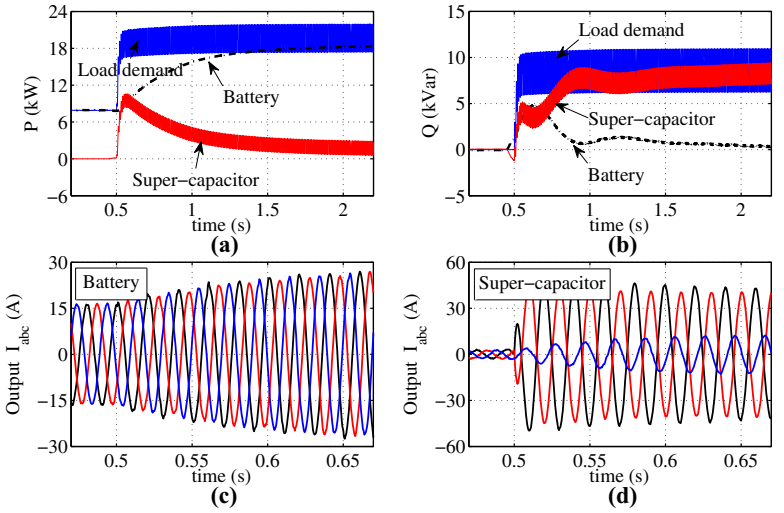

Figure 9.
Comparison of battery and supercapacitor performance in hybrid ESS under single-phase load. (a) Active power output; (b) reactive power output; (c) current output from the battery; (d) current output from the SC

results, the battery accumulated DOD is reduced and efficiency is smoothed due to the help of SC to filter the unbalanced power demand to balanced power demand that reduced the battery internal power loss. To compare the improvement numerically, the indices of control performance of battery ESS and hybrid ESS are shown in Table 3 and the indices are also shown in the bar chart in Figure 12.

It shows that the hybrid ESS using the proposed strategy has faster transient response in bus voltage that leads to less bus voltage drop and integrated absolute error (IAE). From the result, the peak voltage drops on bus maintained by battery ESS is 0.26, while that of hybrid ESS is 0.04, 85% less than that of battery ESS. The voltage IAE of bus maintained by battery ESS is 0.13 while that of hybrid ESS is 0.036. The improve on voltage IAE is about 72%, smaller than that of peak voltage drop. This verifies the effectiveness of using

Indices System	Battery ESS	Hybrid ESS	Improvements
Case 1: single-phase load			
Voltage drop (p.u.)	0.26	0.04	85% less
Voltage IAE	0.13	0.036	72% less
Peak VUF (%)	38.4	3.1	92% less
Average VUF (%)	5.4	1.4	74% less
Power loss (W)	518	269	46% less
Accumulate DOD ($\times 10^{-5}$)	1.7	1.4	17.6% less
Average efficiency (%)	98.9	99.1	0.2% higher
Case 2: Single-phase power generation			
Voltage drop (p.u.)	0.17	0.027	84% less
Voltage IAE	0.10	0.03	70% less
Peak VUF (%)	43	2.2	95% less
Average VUF (%)	6.9	1.4	79% less
Power loss (W)	63	23	64% less
Accumulate DOD ($\times 10^{-5}$)	0.68	0.32	52% less
Average Efficiency (%)	99.4	99.6	0.2% higher

Table 3.
Performance indices of Battery ESS and Hybrid ESS

SC to improve the transient voltage performance. In addition, the unbalance voltage elimination capability of HESS using the proposed control algorithm designed for unbalanced load is obvious better than the battery ESS with less VUF under single-phase load. The reduction of peak VUF and average VUF of hybrid ESS comparing with the battery ESS are 92% and 74%, respectively. For the improvement of battery life cycles, the power loss on battery has reduced about 46% and the accumulated DOD has reduced about 18%. The average efficiency on battery and its VSC is about 0.2% higher due to the unbalanced power is moved to be balanced by SC.

4.3 Case 2: single-phase power generation

The renewable power generation is always unpredictable and changes rapidly referring to weather conditions. It cannot always match the power demand from end-user. Thus, the power difference will be balanced by the ESS. This will cause frequent charge and discharge cycles. If the renewable power generation is small and low power, it normally connected directly to the single-phase of bus voltage. In this case, the performance of battery ESS and hybrid ESS has been compared in Figure 10. Due to the single-phase power generation is time-varying, the bus voltage of battery ESS has obviously worse power quality and unbalanced voltage than the hybrid ESS, as shown in Figures 10a and b. This can also be found in Figures 10c and d that the VUF of hybrid ESS is much lower than that of battery ESS. The indices comparison in Table 3 and Figure 12 show that peak voltage drop of using hybrid ESS is about 84% lower than that of the battery ESS while the voltage IAE reduction

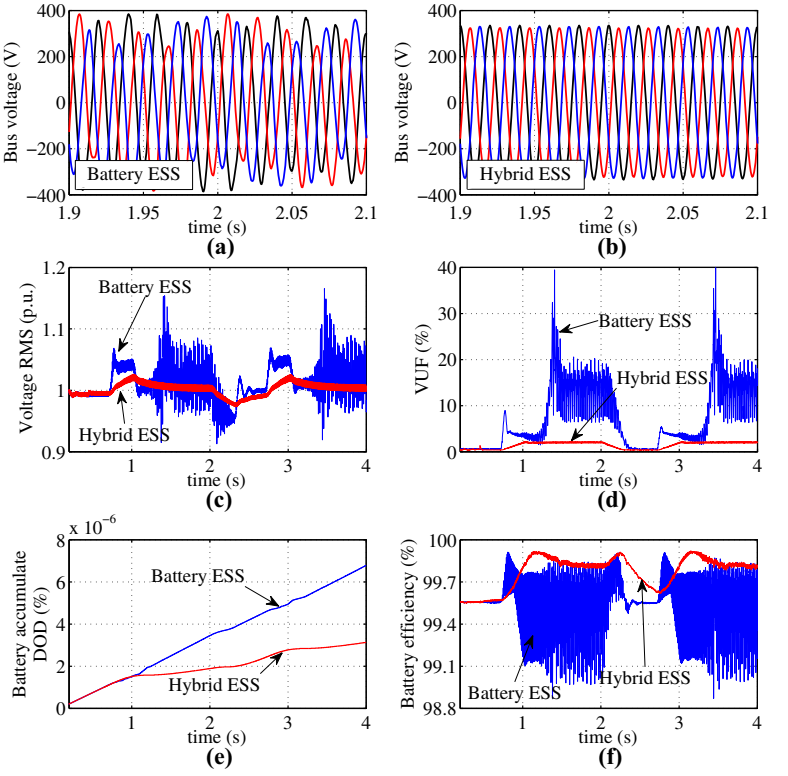

Figure 10.
Simulation comparison between battery ESS and hybrid ESS in a standalone microgrid under single-phase power generation. (a) Bus voltage with battery ESS; (b) bus voltage with hybrid ESS; (c) comparison of RMS bus voltage; (d) bus voltage unbalance factor; (e) battery accumulate DOD; and (f) battery efficiency

is about 70% less. The VUF reduction of bus voltage under single-phase power generation is about 79% in average and 95% for the peak.

The comparison of active power and reactive power generation in hybrid ESS is shown in Figures 11a and b. The battery is controlled to generate averaged and slowly changed active power and zero reactive power in steady state. The output and absorbed current of battery is three-phase balanced while that of SC is unbalanced to support the single-phase load or generation as shown in Figures 11c and d.

The objective of using SC in a HESS is to reduce the usage of battery to increase its lifetime. This is verified in Figure 10e that the battery accumulated DOD of hybrid ESS is much lower than that of battery ESS. In the numerical comparison, the reduction of

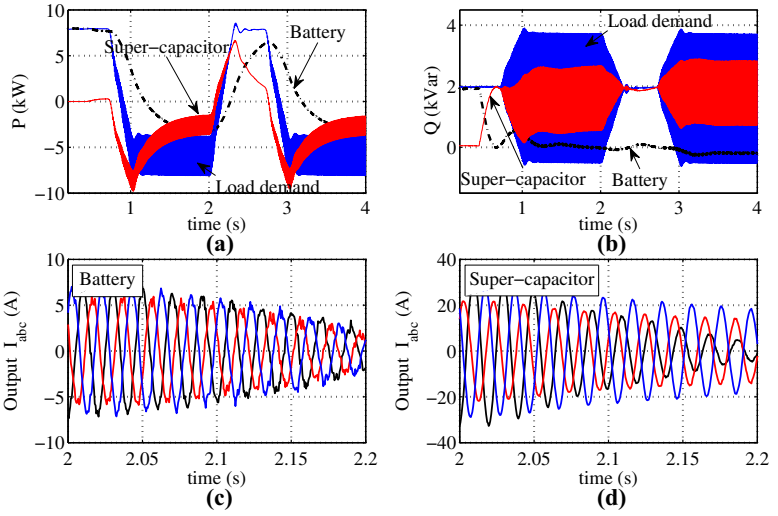

Figure 11.
Comparison of battery and supercapacitor performance in hybrid ESS under single-phase power generation. (a) Active power output; (b) reactive power output; (c) current output from the battery; (d) current output from the SC

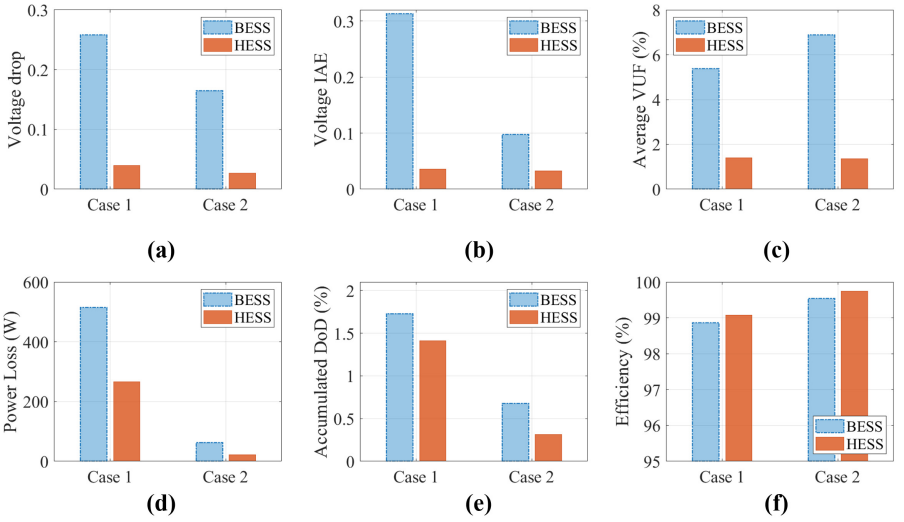

Figure 12.
Indices comparison between BESS and HESS in bus voltage performance of (a) voltage drop, (b) voltage IAE, and (c) average VUF; and battery performance of (d) internal power loss, (e) accumulate DOD, (f) average efficiency

accumulate DOD is about 52% less of using hybrid ESS. The battery efficiency is shown in Figure 10f and shows that it has about 0.2% improvement in average (see Figure 12).

5. Conclusion

This paper proposed an energy management strategy for a battery and supercapacitor (SC) hybrid energy storage system (HESS) in order to improve the transient performance of bus voltage under unbalanced load condition in a standalone AC microgrid (MG) and reduce the usage of battery. The energy management strategy controlled the battery and SC with coordinated design to balance the power demand and generation and maintain the bus voltage. In AC MG, the single-phase load and generation can easily cause the unbalance voltage issue. It not only reduced the power quality but also caused unnecessary power loss in battery to reduce its cycle life. With the proposed energy management strategy, the SC is used to absorb the reactive power and transient and unbalanced active power, while the battery is used to generate balanced power in three phase to the grid to balance the steady state power demand. The energy management strategy of battery/supercapacitor HESS in a standalone AC MG is validated in simulation using PSCAD/EMTDC. The results show that performance of bus voltage under unbalanced disturbance has been improved with faster transient response and less voltage drop. The energy management strategy is suitable for the plug-and-play requirement in standalone MG application with flexible number of SC referring to different operation requirements. The reduction of battery loss has also been validated as lower accumulate DOD and higher average efficiency.

References

Abbey, C. and Joos, G. (2007), "Supercapacitor energy storage for wind energy applications", *IEEE Transactions on Industry Applications*, Vol. 43 No. 3, pp. 769-776, doi: 10.1109/TIA.2007.895768.

Abdelkader, A., Rabeh, A., Ali, D.M. and Mohamed, J. (2018), "Multi-objective genetic algorithm based sizing optimization of a stand-alone wind/pv power supply system with enhanced battery/supercapacitor hybrid energy storage", *Energy*, Vol. 163, pp. 351-363.

Bae, K.c., Choi, S.c., Kim, J.h., Won, C.y. and Jung, Y.c. (2014), "LiFePO4 dynamic battery modeling for battery simulator", *Industrial Technology (ICIT), 2014 IEEE International Conference on*, pp. 354-358, doi: 10.1109/ICIT.2014.6894892.

Bidram, A., Davoudi, A., Lewis, F.L. and Guerrero, J.M. (2013), "Distributed cooperative secondary control of microgrids using feedback linearization", *IEEE Transactions on Power Systems*, Vol. 28 No. 3, pp. 3462-3470, doi: 10.1109/TPWRS.2013.2247071.

Blaabjerg, F., Chen, Z. and Kjaer, S.B. (2004), "Power electronics as efficient interface in dispersed power generation systems", *IEEE Transactions on Power Electronics*, Vol. 19 No. 5, pp. 1184-1194, doi: 10.1109/TPEL.2004.833453.

Blaabjerg, F., Yang, Y. and Ma, K. (2013), "Power electronics - key technology for renewable energy systems - status and future", *Electric Power and Energy Conversion Systems (EPECS), 2013 3rd International Conference on*, pp. 1-6, doi: 10.1109/EPECS.2013.6712980.

Camara, M.B., Gualous, H., Gustin, F. and Berthon, A. (2008), "Design and new control of DC/DC converters to share energy between supercapacitors and batteries in hybrid vehicles", *IEEE Transactions on Vehicular Technology*, Vol. 57 No. 5, pp. 2721-2735, doi: 10.1109/TVT.2008.915491.

Camara, M.B., Gualous, H., Gustin, F., Berthon, A. and Dakyo, B. (2010), "DC/DC converter design for supercapacitor and battery power management in hybrid vehicle applications - polynomial control strategy", *IEEE Transactions on Industrial Electronics*, Vol. 57 No. 2, pp. 587-597, doi: 10.1109/TIE.2009.2025283.

Camara, M.B., Dakyo, B. and Gualous, H. (2012), "Polynomial control method of DC/DC converters for DC-bus voltage and currents management - battery and supercapacitors", *IEEE Transactions on Power Electronics*, Vol. 27 No. 3, pp. 1455-1467, doi: 10.1109/TPEL.2011.2164581.

Chen, H., Zhang, Z., Guan, C. and Gao, H. (2020), "Optimization of sizing and frequency control in battery/supercapacitor hybrid energy storage system for fuel cell ship", *Energy*, Vol. 197, p. 117285.

Diaz, G., Gonzalez-Moran, C., Gomez-Aleixandre, J. and Diez, A. (2009), "Complex-valued state matrices for simple representation of large autonomous microgrids supplied by PQ and Vf generation", *IEEE Transactions on Power Systems*, Vol. 24 No. 4, pp. 1720-1730, doi: 10.1109/TPWRS.2009.2030396.

Dogger, J.D., Roossien, B. and Nieuwenhout, F.D.J. (2011), "Characterization of Li-Ion batteries for intelligent management of distributed grid-connected storage", *IEEE Transactions on Energy Conversion*, Vol. 26 No. 1, pp. 256-263, doi: 10.1109/TEC.2009.2032579.

El-mezyani, T., Wilson, R., Sattler, M., Srivastava, S.K., Edrington, C.S. and Cartes, D.A. (2012), "Quantification of complexity of power electronics based systems", *IET Electrical Systems in Transportation*, Vol. 2 No. 4, pp. 211-222, doi: 10.1049/iet-est.2011.0019.

Enang, C.M. and Johnson, B.K. (2020), "Bidirectional dc-dc converter control in battery-supercapacitor hybrid energy storage system", *2020 IEEE Power and Energy Society Innovative Smart Grid Technologies Conference (ISGT)*, IEEE, pp. 1-5.

Golchoubian, P. and Azad, N.L. (2017), "Real-time nonlinear model predictive control of a battery–supercapacitor hybrid energy storage system in electric vehicles", *IEEE Transactions on Vehicular Technology*, Vol. 66 No. 11, pp. 9678-9688.

Guerrero, J., Vasquez, J., Matas, J., de Vicu, L. and Castilla, M. (2011), "Hierarchical control of droop-controlled AC and DC microgrids - a general approach toward standardization", *IEEE Transactions on Industrial Electronics*, Vol. 58 No. 1, pp. 158-172, doi: 10.1109/TIE.2010.2066534.

Han, Y., Li, Q., Wang, T., Chen, W. and Ma, L. (2017), "Multisource coordination energy management strategy based on soc consensus for a pemfc–battery–supercapacitor hybrid tramway", *IEEE Transactions on Vehicular Technology*, Vol. 67 No. 1, pp. 296-305.

Hu, X., Lin, S., Stanton, S. and Lian, W. (2011), "A foster network thermal model for HEV/EV battery modeling", *IEEE Transactions on Industry Applications*, Vol. 47 No. 4, pp. 1692-1699, doi: 10.1109/TIA.2011.2155012.

Jayasinghe, S.D.G., Vilathgamuwa, D.M. and Madawala, U.K. (2011), "Diode-clamped three-level inverter-based battery/supercapacitor direct integration scheme for renewable energy systems", *IEEE Transactions on Power Electronics*, Vol. 26 No. 12, pp. 3720-3729, doi: 10.1109/TPEL.2011.2148178.

Jing, W., Lai, C.H., Wong, S.H.W. and Wong, M.L.D. (2016), "Battery-supercapacitor hybrid energy storage system in standalone dc microgrids: areview", *IET Renewable Power Generation*, Vol. 11 No. 4, pp. 461-469.

Jing, W., Lai, C.H., Wong, W.S. and Wong, M.D. (2018), "A comprehensive study of battery-supercapacitor hybrid energy storage system for standalone pv power system in rural electrification", *Applied Energy*, Vol. 224, pp. 340-356.

Lasseter, R. (2002), "MicroGrids", *IEEE Power Engineering Society Winter Meeting*, Vol. 1 No. 2002, pp. 305-308, doi: 10.1109/PESW.2002.985003.

Li, W. and Joos, G. (2008), "A power electronic interface for a battery supercapacitor hybrid energy storage system for wind applications", *Power Electronics Specialists Conference, 2008*, IEEE, pp. 1762-1768, PESC 2008, doi: 10.1109/PESC.2008.4592198.

Li, W. and Joos, G. (2008), "A power electronic interface for a battery supercapacitor hybrid energy storage system for wind applications", *2008 IEEE Power Electronics Specialists Conference*, pp. 1762-1768, doi: 10.1109/PESC.2008.4592198.

Li, W., Joos, G. and Belanger, J. (2010), "Real-time simulation of a wind turbine generator coupled with a battery supercapacitor energy storage system", *IEEE Transactions on Industrial Electronics*, Vol. 57 No. 4, pp. 1137-1145, doi: 10.1109/TIE.2009.2037103.

Li, Q., Wang, T., Dai, C., Chen, W. and Ma, L. (2017), "Power management strategy based on adaptive droop control for a fuel cell-battery-supercapacitor hybrid tramway", *IEEE Transactions on Vehicular Technology*, Vol. 67 No. 7, pp. 5658-5670.

Li, L., Planella, F.B., Widanage, W.D. and Marco, J. (2019), "Implementation and model order reduction of a lithium-ion battery single particle model with electrolyte dynamics", *Electrochemical Conference on Energy and the Environment (ECEE 2019): Bioelectrochemistry and Energy Storage* (July 21-26, 2019), ECS.

Maldonado, M.A. and Korba, G.J. (1999), "Power management and distribution system for a more-electric aircraft (madmel)", *IEEE Aerospace and Electronic Systems Magazine*, Vol. 14 No. 12, pp. 3-8, doi: 10.1109/62.811084.

Mao, M., Liu, Y., Jin, P., Huang, H. and Chang, L. (2013), "Energy coordinated control of hybrid battery-supercapacitor storage system in a microgrid", *2013 4th IEEE International Symposium on Power Electronics for Distributed Generation Systems (PEDG)*, pp. 1-6, doi: 10.1109/PEDG.2013.6785596.

Mohamed, Y.A.R.I. and El-Saadany, E.F. (2008), "Adaptive decentralized droop controller to preserve power sharing stability of paralleled inverters in distributed generation microgrids", *IEEE Transactions on Power Electronics*, Vol. 23 No. 6, pp. 2806-2816, doi: 10.1109/TPEL.2008.2005100.

Peas Lopes, J., Moreira, C. and Madureira, A. (2006), "Defining control strategies for MicroGrids islanded operation", *IEEE Transactions on Power Systems*, Vol. 21 No. 2, pp. 916-924, doi: 10.1109/TPWRS.2006.873018.

Ren, Y., Li, S., Jiang, L. and Zeng, P. (2016), "Coordinated control for battery and supercapacitor in hybrid energy storage system in microgrid", *2016 IEEE 8th International Power Electronics and Motion Control Conference (IPEMC-ECCE Asia)*, IEEE, pp. 2654-2660.

Rosero, J.A., Ortega, J.A., Aldabas, E. and Romeral, L. (2007), "Moving towards a more electric aircraft", *IEEE Aerospace and Electronic Systems Magazine*, Vol. 22 No. 3, pp. 3-9, doi: 10.1109/MAES.2007.340500.

Savaghebi, M., Jalilian, A., Vasquez, J. and Guerrero, J. (2013), "Autonomous voltage unbalance compensation in an islanded droop-controlled microgrid", *IEEE Transactions on Industrial Electronics*, Vol. 60 No. 4, pp. 1390-1402, doi: 10.1109/TIE.2012.2185914.

Song, Z., Hou, J., Hofmann, H., Li, J. and Ouyang, M. (2017), "Sliding-mode and lyapunov function-based control for battery/supercapacitor hybrid energy storage system used in electric vehicles", *Energy*, Vol. 122, pp. 601-612.

Song, Z., Li, J., Hou, J., Hofmann, H., Ouyang, M. and Du, J. (2018), "The battery-supercapacitor hybrid energy storage system in electric vehicle applications: a case study", *Energy*, Vol. 154, pp. 433-441.

Thounthong, P., Rael, S. and Davat, B. (2007), "Control strategy of fuel cell and supercapacitors association for a distributed generation system", *IEEE Transactions on Industrial Electronics*, Vol. 54 No. 6, pp. 3225-3233, doi: 10.1109/TIE.2007.896477.

Tremblay, O., Dessaint, L.A. and Dekkiche, A.I. (2007), "A generic battery model for the dynamic simulation of hybrid electric vehicles", *Vehicle Power and Propulsion Conference, 2007*, IEEE, pp. 284-289, VPPC 2007, doi: 10.1109/VPPC.2007.4544139.

Tummuru, N.R., Mishra, M.K. and Srinivas, S. (2015), "Dynamic energy management of hybrid energy storage system with high-gain PV converter", *IEEE Transactions on Energy Conversion*, Vol. 30 No. 1, pp. 150-160, doi: 10.1109/TEC.2014.2357076.

Wheeler, P. and Bozhko, S. (2014), "The more electric aircraft: technology and challenges", *IEEE Electrification Magazine*, Vol. 2 No. 4, pp. 6-12, doi: 10.1109/MELE.2014.2360720.

Yodwong, B., Thounthong, P., Guilbert, D. and Bizon, N. (2020), "Differential flatness-based cascade energy/current control of battery/supercapacitor hybrid source for modern e–vehicle applications", *Mathematics*, Vol. 8 No. 5, p. 704.

Zhang, G., Tang, X. and Qi, Z. (2010), "Research on battery supercapacitor hybrid storage and its application in microgrid", *Power and Energy Engineering Conference (APPEEC), 2010 Asia-Pacific*, pp. 1-4, doi: 10.1109/APPEEC.2010.5448231.

Zhang, Q., Deng, W. and Li, G. (2017), "Stochastic control of predictive power management for battery/supercapacitor hybrid energy storage systems of electric vehicles", *IEEE Transactions on Industrial Informatics*, Vol. 14 No. 7, pp. 3023-3030.

Zhou, H., Bhattacharya, T., Tran, D., Siew, T.S.T. and Khambadkone, A.M. (2011), "Composite energy storage system involving battery and ultracapacitor with dynamic energy management in microgrid applications", *IEEE Transactions on Power Electronics*, Vol. 26 No. 3, pp. 923-930, doi: 10.1109/TPEL.2010.2095040.

Zhu, Y., Zhuo, F. and Wang, F. (2014), "Coordination control of lithium battery-supercapacitor hybrid energy storage system in a microgrid under unbalanced load condition", *Power Electronics and Applications (EPE'14-ECCE Europe), 2014 16th European Conference on*, pp. 1-10, doi: 10.1109/EPE.2014.6910727.

Corresponding author
Lin Jiang can be contacted at: L.Jiang@liverpool.ac.uk